Casein kinase 2-dependent phosphorylation of human Rad9 mediates the interaction between human Rad9-Hus1-Rad1 complex and TopBP1

Takeishi, Yukimasa
Department of Biology, Faculty of Sciences, Kyushu University

Ohashi, Eiji
Department of Biology, Faculty of Sciences, Kyushu University

Ogawa, Kaori
Department of Biology, Faculty of Sciences, Kyushu University

Masai, Hisao
Genome Dynamics Project, Tokyo Metropolitan Institute of Medical Science

他

出版情報：Genes to Cells. 15 (7), pp.761-771, 2010-06. Blackwell Publishing
バージョン：

Casein Kinase 2-dependent phosphorylation of human Rad9 mediates the interaction between human Rad9-Hus1-Rad1 complex and TopBP1

Yukimasa Takeishi[1], Eiji Ohashi[1], Kaori Ogawa[1], Hisao Masai[2], Chikashi Obuse[3] and Toshiki Tsurimoto[1#]

[1]*Department of Biology, School of Sciences, Kyushu University, 6-10-1 Hakozaki, Higashi-ku, Fukuoka 812-8581, Japan*

[2]*Genome Dynamics Project, Tokyo Metropolitan Institute of Medical Science, 2-1-6 Kamikitazawa, Setagaya-ku, Tokyo 156-8506, Japan*

[2]*Faculty of Advanced Life Science, Hokkaido University, Kita-21, Nishi-11, Sapporo, Hokkaido 001-0021, Japan*

[#]Corresponding author: Toshiki Tsurimoto

Tel: +81-92-643-2613, Fax: +81-92-643-2645, E-mail: ttsurimoto@kyudai.jp,

Running title: CK2 phosphorylates 9-1-1 for binding to TopBP1

Total character count: 42,696

ABSTRACT

The checkpoint clamp, Rad9-Hus1-Rad1 (9-1-1) is loaded by the Rad17-RFC complex onto chromatin after DNA damage and plays a key role in the ATR-dependent checkpoint activation. Here, we demonstrate that *in vitro* casein kinase 2 (CK2) specifically interacts with human 9-1-1, and phosphorylates serines 341 and 387 (Ser-341 and Ser-387) in the C-terminal tail of Rad9. Interestingly, phosphorylated Ser-387 has previously been reported to be required for interacting with a checkpoint mediator TopBP1. Indeed, 9-1-1 purified from *Escherichia coli* and phosphorylated *in vitro* by CK2 physically interacts with TopBP1. Further analyses revealed that phosphorylation at both serine residues occurs *in vivo* and are required for the efficient interaction with TopBP1 *in vitro.* Furthermore, when overexpressed in HeLa cells, a mutant Rad9 harboring phospho-deficient substitutions at both Ser-341 and Ser-387 residues causes hypersensitivity to UV and methyl methane sulfonate (MMS). Our observations suggest that CK2 plays a crucial role in the ATR-dependent checkpoint pathway through its ability to phosphorylate Ser-341 and Ser-387 of the Rad9 subunit of the 9-1-1 complex.

INTRODUCTION

ATM (Ataxia telangiectasia mutated) and ATR (ATM- and Rad3- related) are two master regulators of the DNA damage response. Both proteins are members of phosphatidylinositol 3-kinase-related protein kinase (PIKK) family of serine-threonine kinases. While ATM mainly responds to double strand breaks, ATR responds to a wide variety of DNA damage that result in the generation of single-stranded DNA (ssDNA) (Byun et al, 2005; Cimprich & Cortez 2008; Burrow et al, 2008). RPA (Replication Protein A) covers the ssDNA and the ATR-ATRIP (ATR interacting protein) complex is recruited to the damaged site through a direct interaction between ATRIP and RPA (Cortez et al, 2001; Zou & Elledge 2003; Namiki & Zou 2006).

The Rad9-Hus1-Rad1 (9-1-1) clamp is a key complex involved in the activation of the ATR pathway. 9-1-1 forms a ring-shaped heterotrimer, resembling the homotrimeric sliding clamp, PCNA (Shiomi et al, 2002; Griffith et al, 2002; Dore et al, 2009; Xu et al, 2009; Sohn & Cho 2009). PCNA is loaded on DNA by the pentameric RFC complex (RFC_{1-5}), and interacts with numerous proteins involved in DNA replication and repair. Rad17 is another checkpoint protein that shares homology to RFC1 and forms a canonical RFC-like complex with RFC_{2-5} (Rad17-RFC_{2-5}). The 9-1-1 clamp is specifically loaded onto damaged chromatin by Rad17-RFC_{2-5} in an RPA-dependent manner (Bermudez et al, 2003; Zou et al, 2003). While all subunits of the 9-1-1 complex have a PCNA fold, Rad9 has an additional structurally disordered region at its C-terminal tail. The tail is hyperphosphorylated with at least 10 known phosphorylation sites: Ser-272, Ser-277, Thr-292, Ser-328, Ser-336, Ser-341, Thr-355, Ser-375, Ser-380 and Ser-387 (St. Onge et al, 2003, Roos-Mattjus et al, 2003), some of which are phosphorylated upon DNA damage, or as part of the normal cell cycle.

TopBP1 is a mediator protein that bridges two complexes, 9-1-1 and ATR-ATRIP,

which are recruited independently onto damaged chromatin. TopBP1 has eight BRCA1 carboxyl-terminal (BRCT) motifs (Yamane et al, 1997), and has the ATR activation domain between the sixth and seventh BRCT repeats (Kumagai et al, 2006). TopBP1 binds to Rad9 via its N-terminal two BRCT repeats (Mäkiniemi et al, 2001; Greer et al, 2003; St.Onge et al, 2003; Delacroix et al, 2007; Lee et al, 2007) and to the ATR-ATRIP complex via its ATR activation domain (Kumagai et al, 2006; Mordes et al, 2008). It has been reported that the phosphorylation of Rad9 at Ser-387 (Ser-373 of *Xenopus* Rad9) is essential for the interaction between Rad9 and TopBP1 (St.Onge et al, 2003; Delacroix et al, 2007; Lee et al, 2007). However, the kinase(s) responsible for the phosphorylation is unknown and the direct impact of the phosphorylation on the 9-1-1–TopBP1 interaction remains to be studied with purified proteins.

Casein Kinase 2 (CK2) is a highly conserved, ubiquitous and constitutively active Serine/Threonine kinase that phosphorylates a wide variety of substrates (Meggio & Pinna 2003). CK2 holoenzyme consists of two catalytic subunits, α and α' in αα, αα' or α'α' forms, and the dimeric regulatory subunit, ββ. Despite its constitutive activity, CK2 was reported to phosphorylate several regulatory proteins involved in the DNA damage response, such as, p53 (Meek et al, 1990; Herrmann et al, 1991), MDM2 (Guerra et al, 1997), XRCC1 (Loizou et al, 2004), and MDC1 (Melander et al, 2008; Spycher et al, 2008; Chapman & Jackson 2008; Wu et al, 2008).

In this report, we describe a novel role for CK2 in DNA damage response pathway, in which CK2 phosphorylates residues Ser-341 and Ser-387 of human Rad9, both of which promote the interaction between 9-1-1 and TopBP1 *in vitro*. We also demonstrate that HeLa cells overexpressing a mutant Rad9 that could not be phosphorylated at the both CK2 target sites exhibits elevated UV- and MMS-sensitivity. Based upon our observations, we propose that a novel function of CK2 in the ATR-dependent checkpoint pathway is the

phosphorylation of Rad9 that facilitates the interaction between 9-1-1 and TopBP1.

RESULTS

Interaction and phosphorylation of 9-1-1 by CK2-The 9-1-1 complex has been reported to interact with various proteins involved in DNA repair, DNA damage checkpoint, and apoptosis (Parrilla-Castellar et al, 2004). To identify novel proteins that interact with the 9-1-1 complex, we prepared a 9-1-1-conjugated resin with recombinant human 9-1-1 complex as previously described for PCNA-conjugated beads (Ohta et al, 2002). An extract from human 293 cells was applied to the column in 0.1 M NaCl, and proteins binding to the 9-1-1 resin were eluted with 0.3 M NaCl, separated by SDS-PAGE, and subsequently identified by tandem mass spectrometry. Using this approach, we identified various proteins, including CK2α, CK2α', and CK2β, which are components of CK2 complex (Fig. S1). To confirm the interaction between 9-1-1 and CK2, we prepared recombinant human CK2 and 9-1-1 complexes from insect cells (Fig. S2A, B) and studied their co-immunoprecipitation. As shown in Fig. 1A, CK2 efficiently associated with anti-FLAG antibody beads prebound with FLAG-9-1-1, but not in the absence of FLAG-9-1-1. Then we asked whether CK2 would phosphorylate any one of 9-1-1 subunits *in vitro*. Incubation of purified 9-1-1 from *E. coli* with CK2 in the presence of radiolabeled ATP resulted in the incorporation of ^{32}P in Rad9 efficiently and in Rad1 intermediately (Fig. 1B). Any additional phosphorylation of Hus1, or that of control PCNA, could not be detected. It is known that CK2 preferentially phosphorylates serine- or threonine-residues flanked by acidic residues (Meggio & Pinna, 2003). We were therefore able to predict that the potential target residues are Ser-341 and Ser-387 of Rad9 and Ser-280 and Ser-282 of Rad1 (Fig. S3). To test this hypothesis, we overproduced and purified 9-1-1 complexes from *E. coli* with alanine-substitutions in Rad9 at either Ser-341 or Ser-387 alone or in combination (referred to S341A, S387A and 2A, respectively), or in Rad1 at both Ser-280 and Ser-282 (referred to M1) (Fig. S2C) and studied

their phosphorylation by CK2 *in vitro*. Fig. 1C shows that the single substitutions result in a modest reduction in the amount of phosphorylated Rad9. However, the double substitution (2A) completely abolished phosphorylation. Similarly, the M1 mutant of Rad1 was not phosphorylated. Thus, Ser-341 and Ser-387 of Rad9 and Ser-280 and/or Ser-282 of Rad1, are the only 9-1-1 targets of CK2 *in vitro*. We then asked whether CK2 could phosphorylate these residues *in vivo*. To do so, we added a CK2 specific inhibitor, tetrabromocinnamic acid (TBCA) (Pagano et al, 2007) to HeLa cells and monitored *in vivo* phosphorylation of 9-1-1 by immunoblotting of cell lysates with phospho-specific antibodies against Rad9 at Ser-341 or Ser-387 (P-S341 and P-S387) (Fig. 2A). Without TBCA, we could detect protein bands reactive with these antibodies, indicating that S341 and S387 in Rad9 are phosphorylated *in vivo*. However, addition of 200 μM TBCA, which is sufficient to arrest the cell growth, resulted in a reduction in phosphorylation to about 70 % of that observed in the control, suggesting that CK2 has the potential to phosphorylate the Ser-341 and Ser-387 *in vivo*. These values may be underestimated because these antibodies react unphosphorylated Rad9 purified from *E. coli* at about 10% efficiency of the signal with fully phosphorylated residues (Fig. 2B, lane 1).

Phosphorylation of Rad9 by CK2 promotes interaction of 9-1-1 to TopBP1-It has been previously reported that one of the CK2 targets, Ser-387, is essential for the interaction between Rad9 and TopBP1 and plays a crucial role for checkpoint signal activation in human cells (14, 20). Thus, we hypothesized that CK2-dependent phosphorylation of Ser-387 by CK2 would promote an interaction between 9-1-1 and TopBP1. We purified FLAG-tagged 9-1-1 from both insect High Five (9-1-1_HF) and *E. coli* cells (9-1-1_EC) and His-tagged TopBP1 from insect cells (Fig. S2B, C). Rad9 in 9-1-1_HF was highly phosphorylated and its high mobility shift was similar to that observed in human cells (Fig. 2B, C and Fig. S4A). These modifications included phosphorylation at Ser-341 and Ser-387 residues (Fig. 2B, C).

We estimate that roughly 50% of the serine residues were phosphorylated in insect cells, since further treatment of the 9-1-1_HF with CK2 increased the intensity of the phospho-specific bands about two- fold by immunoblotting and incorporated about a half of ^{32}P from that of the 9-1-1_EC by incubation with [γ-^{32}P]ATP (Fig. 2B, lanes 5 and 6; Fig. S4B). Phosphatase treatment of 9-1-1_HF caused the protein to migrate faster during SDS-PAGE and roughly at the same position as the non-phosphorylated 9-1-1_EC. Further treatment with CK2 enhanced the band intensities to the fully phosphorylated level, but the migration of the protein remained unchanged (Fig. 2B, lanes 1-4). Thus, phosphorylation of Rad9 by CK2 did not induce any of its mobility shifts under our conditions.

We used the purified 9-1-1_HF and 9-1-1_EC complexes to study their interaction with TopBP1 using a pull-down assay with Ni-NTA beads. Interestingly, the 9-1-1_HF complex, but not 9-1-1_EC complex, binds to TopBP1 efficiently (Fig. 3A), suggesting that the phosphorylation of 9-1-1 that occurred in insect cells are important for the interaction. 9-1-1_EC was pretreated with CK2 in the presence of ATP, and its ability to bind TopBP1 was similar to the 9-1-1_HF complex. The binding was CK2-phosphorylation specific, since the absence of either ATP, or CK2, reduced binding to background levels (Fig. 3B, lanes 14-16). Thus, the direct interaction between 9-1-1 and TopBP1 was reconstituted through phosphorylation of 9-1-1 with CK2.

Since we added CK2-treated 9-1-1 to the TopBP1-binding assay directly, one could claim that phosphorylation of TopBP1 could occur during the binding assay through the actions of residual amounts of contaminating CK2 (from the 9-1-1 phosphorylation step), and as such, the potential TopBP1 phosphorylation could affect the results. To exclude this possibility, we mixed 9-1-1 and CK2 without ATP first, and only added ATP during the TopBP1-binding assay. As shown in Fig. 3C, lane 12, no interaction was observed, indicating that *de novo* phosphorylation of Rad9 and/or Rad1 with the residual amount of CK2 was

limited and the potential phosphorylation of TopBP1 during the binding step, did not cause the proteins to interact. To further minimize any effects of potential phosphorylation, we added 2 μM TBCA, a concentration to block phosphorylation of Rad9 and Rad1 by CK2 to 10-15% *in vitro* (Fig. S5), prior to adding to the TopBP1-beads. We observed the same level of binding between 9-1-1 and TopBP1 even in the presence of TBCA (Fig. 3C, lanes 10 and 11). Thus, only phosphorylation of Rad9 and/or Rad1 by CK2 is responsible for the interaction between 9-1-1 and TopBP1.

The interaction is dependent on phosphorylation of Ser-341 and Ser-387 of Rad9-To identify the key residue(s) for the interaction, we took advantage of the phospho-deficient mutants of 9-1-1_EC. 9-1-1_ECs containing mutations at the respective CK2 target sites were pre-treated with CK2 and pulled-down by His-TopBP1. S280A and S282A mutations of Rad1 (M1) bound to TopBP1 as efficiently as wild-type (WT) (Fig. 4A, lanes 16 and 18), indicating that the observed minor phosphorylation of Rad1 by CK2 does not contribute to the interaction between 9-1-1 and TopBP1. The M1 mutant of Rad1 cannot be detected by the anti-Rad1 antibody that we used in this experiment, while this mutant complex can be detected by staining with Coomassie Brilliant Blue (compare Fig. 4A, lane 8 and Fig. S2C). In contrast, the S341A and S387A mutants reduced the interaction slightly and significantly, respectively and the 2A mutant completely abolished the interaction (Fig. 4A, lanes 17, 19 and 20). We prepared S387E, and S341E/S387E (2E) mutants to mimic the Rad9 phosphorylated at these serine residues and compared their interactions with TopBP1. Both S387E and 2E mutants exhibited a weak, but significant binding to TopBP1 without CK2 treatment (Fig. 4B). Thus, we could reproduce the phospho-specific binding by phospho-mimicry mutations of Rad9 at Ser-341 and Ser-387. These results indicate that phosphorylation of Ser-387 and Ser-341 by CK2 is necessary and sufficient to allow 9-1-1 to interact with TopBP1.

Both Ser-341 and Ser-387 of Rad9 are important for the DNA damage response-We prepared cell lines expressing WT, S341A, S387A or 2A mutants of Rad9 to test the importance of the CK2-target residues *in vivo*. We introduced plasmids carrying WT or mutant Rad9 cDNAs into HeLa cells and selected stable cell lines that expressed the FLAG-tagged Rad9 proteins at levels of approximately 10-fold greater than the endogenous Rad9 (Fig. 5A). Since the overexpressed Rad9 proteins were incorporated in 9-1-1 complex as similarly as the endogenous one in these HeLa cells (Fig. S6A), it could be expected that approximately 90% of Rad9 in the 9-1-1 complex was substituted with the overexpressed proteins. Their phosphorylation states corresponded to the Rad9 genotype, as indicated by immunoblotting with P-S341 and P-S387 antibodies (Fig. 5A). All the cell lines did not show any growth defects in the absence of DNA damage (Fig. S6B). However, if HeLa cells expressing the 2A Rad9 mutant were treated with UV or MMS, they clearly exhibited decreased cell survival (Fig. 5B, C). In contrast, cell lines expressing either S341A, or S387A single mutants, or WT Rad9 did not exhibit any significant sensitivity. Our observations indicate that both Ser-387 and Ser-341 residues in Rad9, which we identified as the targets of CK2 *in vitro*, are therefore critically important for the DNA damage response in human cells.

DISCUSSION

In this report, we have reconstituted the phospho-dependent 9-1-1–TopBP1 interaction with purified proteins. Our results clearly demonstrate that the interaction is direct, and through the phosphorylation of two serine residues in Rad9 by CK2. Several groups have reported that the phosphorylation of Ser-387 (Ser-373 of *Xenopus* Rad9) is crucial for the interaction with TopBP1 through the use of immunoprecipitation assays and extracts from human cells or frog eggs (St.Onge et al, 2003; Delacroix et al, 2007; Lee et al, 2007). Our *in vitro* results are consistent with the previous reports in that the substitution of Ser-387 with alanine greatly reduces the 9-1-1–TopBP1 interaction. However, we also showed that Ser-341 contributes to the interaction in addition to Ser-387 *in vitro*. Experiments with human cells overexpressing Rad9 mutants demonstrated a more obvious contribution of Ser-341 *in vivo*. It should be noted that the phosphorylation of Ser-341 and Ser-387 were not inter-dependent, since single substitutions of Ser-341 or Ser-387 did not influence the phosphorylation levels of the other serine (Fig. 5A). Thus, the independent phosphorylation events at the two sites may endow a fine-tuning mechanism by which the interaction levels between TopBP1 and 9-1-1 are determined through the extent of their phosphorylation. However, we cannot exclude the possibility that phosphorylation of Ser-341 might play additional roles in the DNA damage response, in addition to TopBP1-binding, so that the Rad9 2A mutant exhibited a synergistic effect on the response *in vivo*.

In our overexpression experiment with Rad9 mutants in HeLa cells, only 2A mutant showed significant sensitivity to UV or MMS. This result was seemingly inconsistent with a previous report (Delacroix et al, 2007), or our own *in vitro* results, because Ser-387 is the predominant determinant of the DNA damage response, or the interaction with TopBP1. However, we believe that this is due to differences in experimental conditions in which we

observed the dominant negative effects of overexpressed Rad9 mutants versus endogenous levels of the Rad9 protein after genotoxic treatments. In our case, we hypothesize that the overexpressed Rad9 2A mutant, which cannot be phosphorylated, is likely to have a much more prominent effect compared to the partially active S341A or S387A mutants. This notion again supports our interpretation that both Ser-341 and Ser-387 are important for interaction with TopBP1.

Our Ala-substitution experiments clearly indicate that the two phospho-serine residues in Rad9 are important for the 9-1-1–TopBP1 interaction. It should be noted that there is a remote possibility that these substitutions may induce structural changes of Rad9 so as to disturb the 9-1-1 trimer formation and subsequently eliminate any protein-protein interactions. However, it has been suggested from the amino acid sequence of Rad9 that the C-terminal highly phosphorylated region would have an extended tail-structure to interact with other proteins (Venclovas & Thelen 2000). Recently, three groups determined the crystal structure of human 9-1-1 without the C-terminal tail region because of its disordered structure, and reported its ring-shaped structure, even without the tail (Dore et al, 2009; Xu et al, 2009; Sohn & Cho 2009). Furthermore, the 9-1-1 trimer structure formed normally with the 2A mutant and even with a mutant with nine alanine substitutions (Fig. S2C and Fig. S6A; Roos-Mattjus et al, 2003). Thus, our Ala-substitutions in Rad9 are unlikely to have strong structural effects, but would instead lead to the absence of the phospho-serine residues at these sites. Indeed, our experiments with phospho-mimic mutants of the same residues, which partially restored the binding activity to TopBP1 without phosphorylation of Rad9 by CK2, support this idea (Fig. 4B). This limited recovery of the interaction by the Glu-substitutions might be due to their local structural effects at the Rad9-TopBP1 interface in addition to their phospho-mimicry function. This point will be addressed in future if their interface structure including the phospho-Ser residues is solved.

While our data strongly supports the hypothesis that CK2 phosphorylates Ser-387 and Ser-341 in Rad9 in human cells, other acidophilic protein kinase(s) are also likely to be involved in its phosphorylation, especially as we observed significant levels of phosphorylated Rad9 in the presence of TBCA (Fig. 2A). For example, a cell cycle regulated kinase, Cdc7/Dbf4 prefers Ser/Thr neighboring acidic residues and would be one potential kinase (Cho et al, 2006). However, much less phosphorylation of human Rad9 occurred with human Cdc7/ASK (human Dbf4) than CK2 *in vitro* (Fig. S7), indicating that the enzyme is unlikely to be a functional kinase for Rad9. Indeed, both Ser-341 and Ser-387 are phosphorylated without DNA damaging treatments and the phosphorylation levels are not significantly changed in HeLa cells (Fig. S8; St. Onge et al, 2003; Roos-Mattjus et al, 2003), which is consistent with the fact that CK2 is a constitutively active kinase. Although CK2 phosphorylates some substrate in a damage-dependent manner, the serine residues in Rad9 were not the case. It has been also reported that the interaction of 9-1-1 and TopBP1, which depends on Rad9-phosphorylation by CK2 as we have demonstrated here, occurs without DNA damage (Mäkiniemi et al, 2001; St. Onge et al, 2003; Greer et al, 2003; Delacroix et al, 2007). Thus, CK2 will be the major kinase responsible for the phosphorylation of Ser-341 and Ser-387 in Rad9, and the resulting interaction of 9-1-1 and TopBP1 will not be under a DNA damage-inducible regulation in human cells. Our notion is again supported by the observation that Chk1 activation in Rad17-deficient DT40 cells could still occur in a DNA damage dependent manner without 9-1-1 loading, if the ATR activation domain of TopBP1 was artificially localized to chromatin (Delacroix et al, 2007). This indicates that 9-1-1–TopBP1 interaction is not necessary for a DNA damage-inducible event during activation of the checkpoint response. Therefore, we propose that phosphorylations at Ser-341 and Ser-387 by CK2 will be a prerequisite of the DNA damage response, and CK2 may “license” the reaction by establishing the binding of TopBP1 to 9-1-1. It has been

reported that 9-1-1 plays more roles than checkpoint activation, especially in DNA repair, as it interacts with its binding partners relating with apoptosis, DNA synthesis and base excision repair (reviewed in Parrilla-Castellar et al, 2004; Lieberman, 2006). If binding of TopBP1 to 9-1-1 hinders interaction with other partners, some populations of 9-1-1 should be kept free for them. The license mechanism will be necessary to sort 9-1-1 into the sub-populations of different functions. Indeed, a certain level of Rad9 is constitutively phosphorylated at Ser-341 and Ser-387 *in vivo* as described above. Thus, CK2 may maintain the level of 9-1-1 sufficient for DNA damage checkpoint response, and the remaining 9-1-1 will adapt to the other functions.

The constitutive phospho-dependent interaction observed here is reminiscent of the MDC1-NBS1 interaction. MDC1 is also constitutively phosphorylated by CK2 and the interaction between MDC1 and NBS1 can be seen in the absence of any DNA damaging treatment (Melander et al, 2008; Spycher et al, 2008; Chapman & Jackson 2008; Wu et al, 2008). NBS1 interacts with phospho-MDC1 via two BRCT motifs and the FHA domain of NBS1. Thus, a common mechanism using CK2 phosphorylation may exist in the two major ATM- and ATR-dependent DNA damage response pathways. Interestingly, any obvious counterparts of the MDC1 or CK2 sites in the C-terminal tail of Rad9 (corresponding to human Rad9 Ser-341 and Ser-387), have not been identified in yeast systems, while the CK2 sites of the Rad9 tail are conserved among vertebrates (Fig. S3). This strongly implies that the CK2-phosphorylation dependent checkpoint response mechanisms may be acquired during the evolution. Further analyses are needed to elucidate the significance of the phosphorylation of Rad9 by CK2 and the cellular mechanism to establish its interaction with TopBP1 during DNA damage responses.

EXPERIMENTAL PROCEDURES

Cell culture, transfection and infection-HeLa cells were cultured in Dulbecco's modified Eagle's medium (DMEM) supplemented with 10% fetal bovine serum (FBS), 100 μg/mL of streptomycin and 100 unit/mL of penicillin at 37˚C in a 5% CO_2 incubator. To obtain cell lines overexpressing WT, or mutant FLAG-Rad9, HeLa cells were transfected with pcDNA3-based plasmids (Invitrogen) carrying these cDNA sequences using FuGENE 6 (Roche). After transfection, stable transformants were selected by adding 400 μg/mL of G418 in the medium. After establishment of the cell lines, 100 μg/mL of G418 was added in the medium to maintain the ectopic expression. Insect High Five cells were cultured in Express five SFM medium (Invitrogen) supplemented with 100 μg/mL streptomycin, 100 unit/mL of penicillin and 2 mM L-glutamine at 27˚C. Baculoviruses were allowed to infect High Five cells ($1.5x10^7$/150 mm dish) for 48-72 h.

Antibodies-Anti-Rad9, Rad17, Polδ, and CK2α antibodies were purchased from Santa Cruz, and anti-penta-His and anti-FLAG-peptide antibodies were from Qiagen and Sigma, respectively. Anti-phospho-Chk1 (P-S317) and Chk2 (P-T68) antibodies were purchased from Cell Signaling Technology. Anti-phospho specific antibodies of Rad9 (P-S341 and P-S387), which could detect the phosphorylated residues specifically as shown in Fig. S4C, lanes 1 and 2, were custom made by Sigma Genosys. Anti-Hus1 and Rad1 antibodies, prepared with their C-terminal oligo peptides, were obtained from Dr. K. Sugimoto (New Jersey Medical School, USA).

Plasmids-pBacPAK8 (Clontech) and pFastBac1 (Invitrogen) were used as baculovirus expression vectors. cDNA fragments of Rad9, Rad1, and Hus1 were obtained as described previously (Shiomi et al 2002) and those of CK2 and TopBP1 were obtained by PCR amplification from a HeLa cell cDNA library (Clontech). For expression of FLAG-9-1-1 in

High Five cells, Rad9, Hus1, and Rad1 cDNA fragments were inserted into pBacPAK8 individually as described previously (Shiomi et al 2002). FLAG epitope cassette (Shiomi et al 2002) was inserted into the *Bam*HI site of the pBacPAK8-Rad9 flanking the start codon of Rad9, to express FLAG-tagged Rad9. To express FLAG-9-1-1 in *E. coli*, the cDNA of Hus1, Rad1, and FLAG-Rad9 were inserted into the pET20b vector (Merck) tandemly in this order. For expression of CK2 in High Five cells, CK2α, α' or His-tagged CK2β cDNA fragment was inserted into the *Bam*HI-*Not*I, *Stu*I-*Not*I, or *Bam*HI-*Not*I sites of pFastBac1, respectively. TopBP1 cDNA fragment was inserted into the *Bam*HI-*Not*I sites of pFastBac1 and 6xHis-cassette was inserted into the *Bam*HI site of the pFastBac1-TopBP1 flanking the start codon of TopBP1.

Purification of 9-1-1 and CK2-For purification of 9-1-1_EC, *E. coli* Rosetta cells carrying the pET20b-based plasmid (Merck) to express FLAG-Rad9, Rad1, and Hus1 were grown in LB to stationary phase and collected cells were lysed by sonication in buffer H (25 mM Hepes-NaOH, pH 8.1, 1 mM EDTA, 0.01% NP40, 10% glycerol and 1 mM PMSF) containing 0.15 M NaCl, and clarified by centrifugation at 30,000 rpm for 30 min at 4˚C. The supernatant was loaded onto a DEAE sepharose column (GE Healthcare, 20 mL) in buffer H containing 0.1 M NaCl, and eluted with buffer H containing 0.4 M NaCl. The eluted fraction was loaded onto an anti-FLAG antibody column (Sigma, 1 mL) in buffer H containing 0.4 M NaCl, washed with buffer H containing 0.1 M NaCl, and eluted with the same buffer containing 100 μg/ml of FLAG peptide (Sigma). The eluted protein pool was loaded onto a mono-Q column (GE Healthcare) and eluted in a 0.1 to 0.6 M NaCl gradient in buffer H, and further purified by sedimentation in a 15-35% glycerol gradient in buffer H containing 0.1 M NaCl at 49,000 rpm for 20 h in an SW50.1 rotor (Beckman).

For purification of 9-1-1_HF, the High Five cells were co-infected with baculoviruses harboring FLAG-Rad9, Rad1, or Hus1 and were lysed in buffer B (50 mM Tris-HCl, pH 7.9,

1 mM EDTA, 10% glycerol, 0.5% NP40, 1 mM PMSF and 20 μg/mL Leupeptin) containing 0.15 M NaCl, and clarified by centrifugation at 30,000 rpm for 15 min at 4˚C. The supernatant was loaded onto a Q-sepharose column (GE Healthcare, 20 mL) in buffer H containing 0.15 M NaCl, and eluted successively with buffer H containing 0.2 M and 0.3M NaCl. The 0.3 M NaCl eluted protein pool was loaded onto an IgG column (1 mL) and the flow through was loaded onto an anti-FLAG antibody column (1 mL) in buffer H containing 0.1 M NaCl and eluted with the same buffer containing 100 μg/ml of FLAG peptide. The eluted protein fraction was loaded onto a Mini Q PC 3.2/3 column (GE Healthcare) and eluted with a 0.1 to 0.6 M NaCl gradient in buffer H.

For purification of CK2, the High Five cells co-infected with baculoviruses harboring CK2α, CK2α', and His-tagged CK2β were lysed in buffer B containing 0.2 M NaCl, and clarified by centrifugation at 30,000 rpm for 15 min at 4˚C. The supernatant was loaded onto a DEAE sepharose column (1 mL) in buffer H containing 0.1 M NaCl, and the bound proteins were eluted with buffer H containing 0.4 M NaCl. The eluted pool was loaded onto a Ni-NTA column (1 mL) pre-equilibrated with buffer A (20 mM Tris-HCl, pH 7.9, 0.1% NP40, 10% glycerol, 0.5 M NaCl, 0.1 mM PMSF and 2 μg/mL Leupeptin) and eluted by 7 ml steps of buffer A containing 5, 20, 50, 100, and 200 mM imidazole. The protein pool eluted with 100 and 200 mM imidazole was loaded onto a mono-Q column in buffer H containing 0.1 M NaCl and eluted by a 0.1-0.6 M NaCl gradient in buffer H.

Binding of 9-1-1 to TopBP1-A High Five cell lysate expressing His-TopBP1 was mixed with Ni-NTA magnetic beads (Qiagen) in buffer C (20 mM Tris-HCl, pH 8.0, 0.1% NP40, 10% glycerol, 0.1 mM PMSF, and 2 μg/mL Leupeptin) containing 0.5 M NaCl and 20 mM imidazole, and the beads immobilized with approximately 400 ng of His-TopBP1 were obtained. 480 ng of purified 9-1-1 was incubated with the His-TopBP1 beads at 4˚C for 2 h in 20 μL of buffer C containing 0.15 M NaCl, followed by 5 washes with binding buffer C

containing 0.2 M NaCl. The bound proteins were eluted by boiling in SDS sample buffer and were analyzed by immunoblotting with indicated antibodies.

Binding of 9-1-1 to CK2-Purified CK2 and FLAG-tagged 9-1-1 were incubated in 20 μL of buffer H containing 0.1 M NaCl for 2 h followed by incubation with FLAG-antibody beads (Sigma) for 1 h. The bound proteins were analyzed by immunoblotting with indicated antibodies.

Phosphorylation of 9-1-1 with CK2-The indicated amounts of CK2 were incubated with 140 ng of 9-1-1_EC or 100 ng of PCNA, for 1 h at 30˚C in 5 μL of CK2 reaction buffer (20 mM Tris-HCl, pH 7.5, 50 mM KCl, 10 mM $MgCl_2$) supplemented with 0.2 mM of [γ-^{32}P]ATP. The reacted proteins were subjected to SDS-PAGE, followed by autoradiography. For phospho-dependent binding assays, 1.2 μg of 9-1-1_EC was phosphorylated with 5 ng of CK2 in 10 μL of CK2 reaction buffer for 1 h at 30˚C.

Cell survival against UV and MMS treatments-Cell survival was measured with the Cell Counting Kit 8 (DOJINDO) according to the manufacturer's instructions with some modifications. Briefly, 2.0 x 10^3 cells per wells were inoculated in 96-well plates and adhered for 24 h. The cells were treated with UV at the indicated doses, or with MMS at indicated concentrations, for 24 h. Seventy-two, or 48 h, after the treatment, surviving cells were determined by the addition of 5 μL of Cell Counting Kit 8 solution containing WST-8 formazan (Ishiyama et al. 1997). The OD_{450} nm was measured with a Multiskan FC (Thermo) after a 2 h and 4 h chromogenic reaction at 37˚C.

ACKNOWLEDGEMENTS

We thank Dr. Roger Woodgate (NICHD, NIH, USA) for his critical reading of this paper and valuable comments. We also thank Mr. Tatsuya Kasugaya and Mr. Nao Mori (Kyushu Univ., Japan) for their contributions to the early stage of this work. We are grateful to Ms. Aya Shinozaki (NAIST, Japan) for her help of the initial mass spectrometric analysis. This study was supported by grants-in-aids from the Ministry of Education, Culture, Sports, Science and Technology of Japan.

REFERENCES

Bermudez, V. P., Lindsey-Boltz, L. A., Cesare, A. J., Maniwa, Y., Griffith, J. D., Hurwitz, J. & Sancar, A. (2003) Loading of the human 9-1-1 checkpoint complex onto DNA by the checkpoint clamp loader hRad17-replication factor C complex *in vitro*. *Proc. Natl. Acad. Sci. USA* **100**, 1633–1638

Burrows, A. E. & Elledge, S. J. (2008) How ATR turns on: TopBP1 goes on ATRIP with ATR. *Genes Dev.* **22**, 1416–1421

Byun, T. S., Pacek, M., Yee, M. C., Walter, J. C. & Cimprich, K. A. (2005) Functional uncoupling of MCM helicase and DNA polymerase activities activates the ATR-dependent checkpoint. *Genes Dev.* **19**, 1040–1052

Chapman, J. R. & Jackson, S. P. (2008) Phospho-dependent interactions between NBS1 and MDC1 mediate chromatin retention of the MRN complex at sites of DNA damage. *EMBO Rep.* **9**, 795-801

Cho, W. H., Lee, Y. J., Kong, S. I., Hurwitz, J. & Lee, J. K. (2006) CDC7 kinase phosphorylates serine residues adjacent to acidic amino acids in the minichromosome maintenance 2 protein. *Proc. Natl. Acad. Sci. USA* **103**, 11521–11526

Cimprich, K. A. & Cortez, D. (2008) ATR: an essential regulator of genome integrity. *Nat. Rev. Mol. Cell Biol.* **9**, 616–627

Cortez, D., Guntuku, S., Qin, J. & Elledge, S. J. (2001) ATR and ATRIP: partners in checkpoint signaling. *Science* **294**, 1713–1716

Delacroix, S., Wagner, J. M., Kobayashi, M., Yamamoto, K. & Karnitz, L. M. (2007) The Rad9-Hus1-Rad1 (9-1-1) clamp activates checkpoint signaling via TopBP1. *Genes Dev.* **21**, 1472–1477

Dore, A. S., Kilkenny, M., Rzechorzek , N. J. & Pearl, L. H. (2009) Crystal structure of the human Rad9-Rad1-Hus1 DNA damage checkpoint complex–Implications for clamp loading and regulation. *Mol. Cell* **34**, 735-745

Greer, D. A., Besley, B. D., Kennedy, K. B. & Davey, S. (2003) hRad9 rapidly binds DNA containing double-strand breaks and is required for damage-dependent topoisomerase II ® binding protein 1 focus formation. *Cancer Res.* **63**, 4829-4835

Griffith, J. D., Lindsey-Boltz, L. A. & Sancar, A. (2002) Structures of the human Rad17-replication factor C and checkpoint Rad 9-1-1 complexes visualized by glycerol spray/low voltage microscopy. *J. Biol. Chem.* **277**, 15233-15236

Guerra, B., Götz, C., Wagner, P., Montenarh, M. & Issinger, O. G. (1997) The carboxy terminus of p53 mimics the polylysine effect of protein kinase CK2-catalyzed MDM2 phosphorylation. *Oncogene* **14**, 2683-2688

Herrmann, C. P., Kraiss, S. & Montenarh, M. (1991) Association of casein kinase II with immunopurified p53. *Oncogene* **6**, 877-884

Ishiyama, M., Miyazono, Y., Sasamoto, K., Ohkura, Y. & Ueno, K. (1997) A highly water-soluble disulfonated tetrazolium salt as a chromogenic indicator for NADH as well as cell viability. *Talanta* **44**, 1299-1305

Kumagai, A., Lee, J., Yoo, H. Y. & Dunphy, W. G. (2006) TopBP1 activates the ATR-ATRIP complex. *Cell* **124**, 943–955

Lee, J., Kumagai, A. & Dunphy, W. G. (2007) The Rad9-Hus1-Rad1 checkpoint clamp regulates interaction of TopBP1 with ATR. *J. Biol. Chem.* **282**, 28036–28044

Lieberman, H. B. (2006) Rad9, an evolutionarily conserved gene with multiple functions for preserving genomic integrity. *J Cell. Biochem.* **97**, 690-697

Loizou, J.I., El-Khamisy, S.F., Zlatanou, A., Moore, D.J., Chan, D.W., Qin, J., Sarno, S., Meggio, F., Pinna, L.A. & Caldecott, K.W. (2004) The protein kinase CK2 facilitates repair of chromosomal DNA single-strand breaks. *Cell* **117**, 17-28

Mäkiniemi, M., Hillukkala, T., Tuusa, J., Reini, K., Vaara, M., Huang, D., Pospiech, H., Majuri, I., Westerling, T., Mäkelä, T. P. & Syväoja, J. E. (2001) BRCT domain-containing protein TopBP1 functions in DNA replication and damage response. *J. Biol. Chem.* **276**, 30399-30406

Meggio, F. & Pinna, L.A. (2003) One-thousand-and-one substrates of protein kinase CK2? *FASEB J.* **17**, 349-368

Meek, D. W., Simon, S., Kikkawa, U. & Eckhart, W. (1990) The p53 tumour suppressor protein is phosphorylated at serine 389 by casein kinase II. *EMBO J.* **9**, 3253-3260

Melander, F., Bekker-Jensen, S., Falck, J., Bartek, J., Mailand, N. & Lukas, J. (2008) Phosphorylation of SDT repeats in the MDC1 N terminus triggers retention of NBS1 at the DNA damage-modified chromatin. *J. Cell Biol.* **181**, 213-226

Mordes, D.A., Glick, G.G., Zhao, R. & Cortez, D. (2008) TopBP1 activates ATR through ATRIP and a PIKK regulatory domain. *Genes Dev.* **22**, 1478–1489

Namiki, Y. & Zou, L. (2006) ATRIP associates with replication protein A-coated ssDNA through multiple interactions. *Proc. Natl. Acad. Sci. USA* **103**, 580–585

Ohta, S., Shiomi, Y., Sugimoto, K., Obuse, C. & Tsurimoto, T. (2002) A proteomics approach to identify proliferating cell nuclear antigen (PCNA)-binding proteins in human cell lysates. Identification of the human CHL12/RFCs2-5 complex as a novel PCNA-binding protein. *J. Biol. Chem.* **277**, 40362-40367

Parrilla-Castellar, E.R., Arlander, S.J. & Karnitz, L. (2004) Dial 9-1-1 for DNA damage: the Rad9-Hus1-Rad1 (9-1-1) clamp complex. *DNA Repair* **3**, 1009–1014

Pagano, M.A., Poletto, G., Di Maira, G., Cozza, G., Ruzzene, M., Sarno, S., Bain, J., Elliott, M., Moro, S., Zagotto, G., Meggio, F. & Pinna, L.A. (2007) Tetrabromocinnamic acid

(TBCA) and related compounds represent a new class of specific protein kinase CK2 inhibitors. *Chembiochem* **8**, 129-139

Roos-Mattjus, P., Hopkins, K. M., Oestreich, A. J., Vroman, B. T., Johnson, K. L., Naylor, S., Lieberman, H. B. & Karnitz, L. M. (2003) Phosphorylation of human Rad9 is required for genotoxin-activated checkpoint signaling. *J. Biol. Chem.* **278**, 24428-24437

Shiomi, Y., Shinozaki, A., Nakada, D., Sugimoto, K., Usukura, J., Obuse, C. & Tsurimoto, T. (2002) Clamp and clamp loader structures of the human checkpoint protein complexes, Rad9-1-1 and Rad17-RFC. *Genes Cells* **7**, 861-868

Sohn, S. Y. & Cho, Y. (2009) Crystal structure of the human Rad9-Hus1-Rad1 clamp. *J. Mol. Biol.* **390**, 490-502

Spycher, C., Miller, E. S., Townsend, K., Pavic, L., Morrice, N. A., Janscak, P., Stewart, G. S. & Stucki, M. (2008) Constitutive phosphorylation of MDC1 physically links the MRE11-RAD50-NBS1 complex to damaged chromatin. *J. Cell Biol.* **181**, 227-240

St. Onge, R. P., Besley, B. D., Pelley, J. L. & Davey, S. (2003) A role for the phosphorylation of hRad9 in checkpoint signaling. *J. Biol. Chem.* **278**, 26620-26628

Venclovas, C. & Thelen, M. P. (2000) Structure-based predictions of Rad1, Rad9, Hus1 and Rad17 participation in sliding clamp and clamp-loading complexes. *Nucleic Acids Res.* **28**, 2481-2493

Wu, L., Luo, K., Lou, Z. & Chen, J. (2008) MDC1 regulates intra-S-phase checkpoint by targeting NBS1 to DNA double-strand breaks. *Proc. Natl. Acad. Sci. USA* **105**, 11200-11205

Xu, M., Bai, L., Gong, Y., Xie, W., Hang, H. & Jiang, T. (2009) Structure and functional implications of the human Rad9-Hus1-Rad1 cell cycle checkpoint complex. *J. Biol. Chem.* **284**, 20457-20461

Yamane, K., Kawabata, M. & Tsuruo, T. (1997) A DNA-topoisomerase-II-binding protein with eight repeating regions similar to DNA-repair enzymes and to a cell cycle regulator. *Eur. J. Biochem.* **250**, 794-799

Zou, L. & Elledge, S. J. (2003) Sensing DNA damage through ATRIP recognition of RPA-ssDNA complexes. *Science* **300**, 1542–1548

Zou, L., Liu, D. & Elledge, S. J. (2003) Replication protein A-mediated recruitment and activation of Rad17 complexes. *Proc. Natl. Acad. Sci. USA* **100**, 13827–13832

FIGURE LEGENDS

Figure 1. CK2 binds to and phosphorylates the 9-1-1 complex. (*A*) Co-immunoprecipitation of FLAG-9-1-1 and CK2 holoenzyme. Purified FLAG-9-1-1 complex (1.5 μg) and CK2 holoenzyme (390 ng) were co-immunoprecipitated with anti-FLAG-antibody and immunoblotted with anti-CK2α antibody. Fifty-fold excess of bound (BD; lanes 5 and 6) fractions vs. input (IN; lanes 1 and 2), or unbound (UB; lanes 3 and 4) fractions were applied for analysis. (*B*) Phosphorylation of 9-1-1 with CK2. 9-1-1 _EC (lanes 1-4), or PCNA (lanes 5-8) were incubated with [γ-^{32}P]ATP and CK2 (0 ng, lanes 1 and 5; 0.6 ng, lanes 2 and 6; 3.2 ng, lanes 3 and 7; 16 ng, lanes 4 and 8). Asterisks represent autophosphorylated CK2β. (*C*) Phosphorylation of Ser-341 and Ser-387 of Rad9 and Ser-280 and/or Ser-282 of Rad1 by CK2. 9-1-1 complexes containing WT (lane 2), Rad9 mutants S341A, S387A, or 2A, or Rad1 mutant M1 (lanes 3-6), or PCNA (lane 1) were treated with CK2 as in (*B*).

Figure 2. CK2 phosphorylates Rad9 in HeLa and insect cells. (*A*) Effects of TBCA on phosphorylation of Rad9 at Ser-341 and Ser-387 in HeLa cells. Cells were treated with 200 μM of TBCA for 48 h and phosphorylation levels of the residues were analyzed with their phospho-peptide specific antibodies. Total Rad9, or those phosphorylated at Ser-341, or at Ser-387, were detected with anti-Rad9 (left), P-S341 (middle), or P-S387 (right), respectively, and their relative band intensities with (+), or without (-), TBCA were quantified with Image Gauge software, followed by normalization with those of Polδ. Values are the means of at least three independent experiments and error bars are ±SEM. (*B*) 9-1-1_HF is highly phosphorylated at Ser-341 and Ser-387. 9-1-1_EC (lanes 1 and 2), or 9-1-1_HF before (lanes 5 and 6), or after (lanes 3 and 4) incubation with λPPase, was further purified by glycerol gradient sedimentation. The peak fractions were incubated with (lanes 2, 4 and 6),

or without (lanes 1, 3 and 5) CK2, and immunoblotted with the indicated antibodies. (*C*) 9-1-1_HF (lane 1) and the FLAG-Rad9 expressed in HeLa cells after immunoprecipitation with anti-FLAG antibody (lane 2) were immunoblotted with the indicated antibodies.

Figure 3. 9-1-1 complex phosphorylated by CK2 binds to TopBP1. The input (IN; lanes 1-4 (*A*), lanes 1-8 (*B*), lanes 1-6(*C*)) and bound (BD; lanes 5-8 (*A*), lanes 9-16 (*B*), lanes 7-12 (*C*)) proteins were detected with indicated antibodies. Fifty- (*A*) or 20- (*B, C*) fold excess of the bound fractions vs. the input were applied for the analysis. (*A*) 9-1-1 complex purified from insect cells binds to TopBP1. His-TopBP1 was immobilized on Ni-NTA beads and mixed with 9-1-1_HF (H, lanes 1, 3, 5 and 7) or 9-1-1_EC (E, lanes 2, 4, 6 and 8). (*B*) 9-1-1 purified from *E. coli* binds to TopBP1 after phosphorylation by CK2. 9-1-1_EC (1.2 μg) was mixed with (+), or without (-), ATP and purified CK2 (5 ng). Aliquots of the reaction mixtures (0.48 μg of 9-1-1), or 9-1-1_HF were mixed with Ni-NTA beads with (+), or without (-), prebound His-TopBP1 (0.4 μg). (*C*) Possible de novo-phosphorylation of TopBP1 during the binding assay does not affect protein binding. ATP was added to the reaction mixture containing purified 9-1-1_EC and CK2 before (B, lanes 1, 2, 4, 5, 7, 8, 10, and 11) or after (A, lanes 3, 6, 9, and 12) incubation at 37˚C, and aliquots of the reacted mixtures were incubated with Ni-NTA beads with (+), or without (-), prebound His-TopBP1 in the presence (+), or absence (-), of 2 μM TBCA.

Figure 4. Ser-341 and Ser-387 are important for the interaction with TopBP1. Aliquots of the CK2 reaction mixtures were mixed with Ni-NTA beads with (+), or without (-), prebound His-TopBP1. Input (IN; lanes 1-10 (*A*), lanes 1-8 (*B*)) and bound (BD; lanes 11-20 (*A*), lanes 9-16 (*B*)) proteins were detected with the indicated antibodies. Twenty-fold excess of the bound fractions vs. input was applied for the analysis. (*A*) The phospho-null Rad9 mutant,

2A does not bind to TopBP1. 9-1-1 complexes containing WT Rad9 or Rad9 mutants as indicated, were mixed with ATP and purified CK2. The protein bands of M1 mutant did not appear in lanes 3, 8 and 17, due to inability of the used anti-Rad1 antibody to react with the mutant Rad1. The used 9-1-1 of M1 did contain Rad1 as shown by Coomassie Brilliant Blue staining (Fig. S2C, lane M1). (*B*) The phospho-mimic Rad9 mutants, S387E and 2E bound to TopBP1 without phosphorylation by CK2. Purified WT, or mutant 9-1-1 complexes, from *E. coli* were mixed with (lanes 1, 5, 9, and 13) or without (lanes 2-4, 6-8, 10-12, and 14-16) ATP in the presence of purified CK2.

Figure 5. Cells overexpressing the phospho-null Rad9 mutant, 2A are UV- and MMS-sensitive. (*A*) Overexpression of Rad9 in HeLa cells. Rad9 and phosphorylated Rad9 were detected with an equivalent amount of cell lysate with the indicated antibodies. (*B, C*) Survival after UV- or MMS-treatment. HeLa cells (diamonds), HeLa cells expressing WT (squares) or S341A (circles, dashed line), S387A (pluses, dashed line), or 2A (triangles) were treated with UV (*B*) or MMS (*C*) and the number of surviving cells were determined (see EXPERIMENTAL PROCEDURES). Values are the means of at least three independent experiments and error bars are ±SEM.

Supplementary Figure Legends

Fig. S1. Identification of the 9-1-1 interacting proteins. A human cell nuclear extract was applied onto BSA (left lane) or 9-1-1 (right lane) columns. Bound proteins were eluted with 0.3 M NaCl, separated by SDS-PAGE and stained with Coomassie Brilliant Blue (left panel). The gel was cut into 60 pieces and proteins were identified by mass-spectrometric analyses. The graphs in the middle of the figure indicate the number of identified peptide hits (abscissa) of TopBP1, RFC5, CK2α, CK2α', and CK2β in the gel slices (vertical axes, from the top to bottom). Rad17 was identified in the 9-1-1 eluate specifically (right panel) only by immunoblotting with anti-Rad17 antibody. 10 μL of the extract (Load), 10 μL of the flow through fraction (Unbound), 15 μL of the BSA eluate (BSA) and 15 μL of the 9-1-1 eluate (9-1-1) were used.

Fig. S2. Purified proteins used in this work (CK2 (*A*), 900 ng; TopBP1 (*B*), 400 ng; 9-1-1_HF (*B*), 540 ng; 9-1-1_ECs (*C*), 1.0 μg of WT and mutant protein. Proteins were subjected to 12.5% SDS-PAGE, followed by staining with Coomassie Brilliant Blue.

Fig. S3. Alignment of the amino acid sequences of Rad9 from several organisms and the sequence of human Rad1. ClustalW2 software (http://www.ebi.ac.uk/Tools/clustalw2/index.html) was used for the alignment. Serines and threonines are shown in blue and acidic residues are shown in red. hs, *Homo sapiens*; mm, *Mus musculus*; xl, *Xenopus laevis*; gg, *Gallus gallus*; sp, *Schizosaccharomyces pombe*; sc, *Saccharomyces cerevisiae*.

Fig. S4. Rad9 in High Five cells are highly phosphorylated. (*A*) 9-1-1_HF (150 ng) was incubated with increasing amounts of λPPase (lanes 1-5 are 0, 0.1, 0.5, 2.5 and 12.5 unit, respectively) and subjected to SDS-PAGE, followed by staining with Coomassie Brilliant Blue. (*B*) Phosphorylation of 9-1-1_HF and 9-1-1_EC(P) with CK2. 0.5 μg of 9-1-1_HF (lanes 1-5) or 9-1-1_EC(P) (*E. coli* expressed FLAG-9-1-1 with Rad1 tagged with ProteinC peptide) (lanes 6-10) were incubated with [γ-^{32}P]ATP and 10 units of CK2, and one tenth of the samples were withdrawn at indicated times and analyzed by autoradiography. Band positions of FLAG-Rad9 and Rad1 with (lanes 6-10) or without (lanes 1-5) ProteinC-tag were indicated. Their band intensities were measured and ratios of Rad9/Rad1 were indicated

at bottom.

Fig. S5. CK2-dependent phosphorylation of 9-1-1 complex was inhibited by TBCA. (*A*-*C*) 9-1-1_EC (lanes 1-5), or PCNA (lanes 6 and 7), were incubated with 0.2 mM of [γ-^{32}P]ATP and 5 ng of CK2 (+ or -) in the presence of TBCA (lanes 1-5 are 0, 0.1, 0.5, 1 and 2 μM, respectively). Samples were analyzed by 12.5% SDS-PAGE followed by autoradiography. Graphs in *B* and *C* indicate the relative band intensities quantified with ImageGauge software (vertical axes) against TBCA concentrations (abscissa).

Fig. S6. Characterization of cell lines overexpressing WT, or mutants of Rad9. (*A*) Overexpressed FLAG-Rad9 in HeLa cells forms complex with Rad1 and Hus1. 5.0 x 10^6 of HeLa cells overexpressing WT or mutant Rad9s were lysed in 100 μL of buffer H (see Materials and Methods), and FLAG-Rad9 in the lysates were immunoprecipitated with anti-FLAG-antibody and immunoblotted with indicated antibodies. 3.3-fold excess of immunoprecipitated (IP) fractions vs. input fractions were applied for analysis. Rad1 and Hus1 were efficiently co-precipitated. (*B*) Cell lines overexpressing WT, or mutants of Rad9, grow normally. 2.5 x 10^4 cells were inoculated in 35 mm dishes and incubated at 37˚C and 5% CO_2. Cell numbers were counted with a hemocytometer every 24 h for 6 days using the trypsinized cells.

Fig. S7. Phosphorylation of Rad9 with Cdc7-ASK and CK2. 250 ng of 9-1-1_EC was incubated with [γ-^{32}P]ATP and 204 ng of Cdc7/ASK (lanes 1, 3) or 75 ng of CK2 (lanes 2, 3) at 30 ˚C for 30 min, and analyzed by autoradiography (*A*) and immunoblotting with P-S341 (upper) or P-S387 (lower) antibodies (*B*). Arrows and asterisks represent autophosphorylated GST-Cdc7, phosphorylated FLAG-Rad9, Rad1 and autophosphorylated CK2α and β as indicated.

Fig. S8. Phosphorylation levels of Rad9 at Ser-341 and Ser-387 are unchanged before and after DNA damaging treatments. HeLa cells were treated with UV (50 J/m^2, lanes 2-5), HU (10 mM, lanes 7-10) and MMS (200 μg/mL, lanes 12-15) or left untreated (lanes 1, 6, and 11). After the indicated times of incubation, cells were collected and phosphorylation levels were analyzed by immunoblotting using indicated antibodies.

Fig. 1

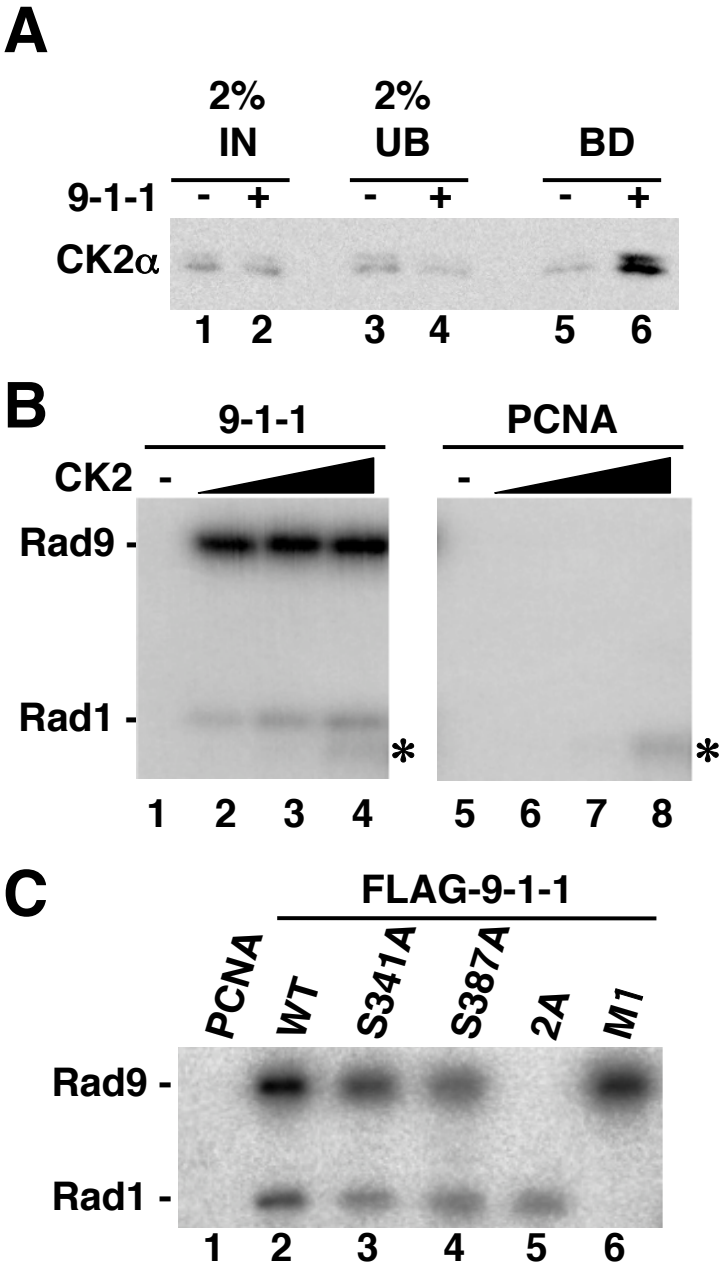
A
2%
IN
2%
UB
BD
9-1-1
- + - + - +
CK2α
1 2 3 4 5 6
B
9-1-1
PCNA
CK2 -
-
Rad9 -
Rad1 -
*
*
1 2 3 4 5 6 7 8
C
FLAG-9-1-1
PCNA
WT
S341A
S387A
2A
M1
Rad9 -
Rad1 -
1 2 3 4 5 6

Fig. 2

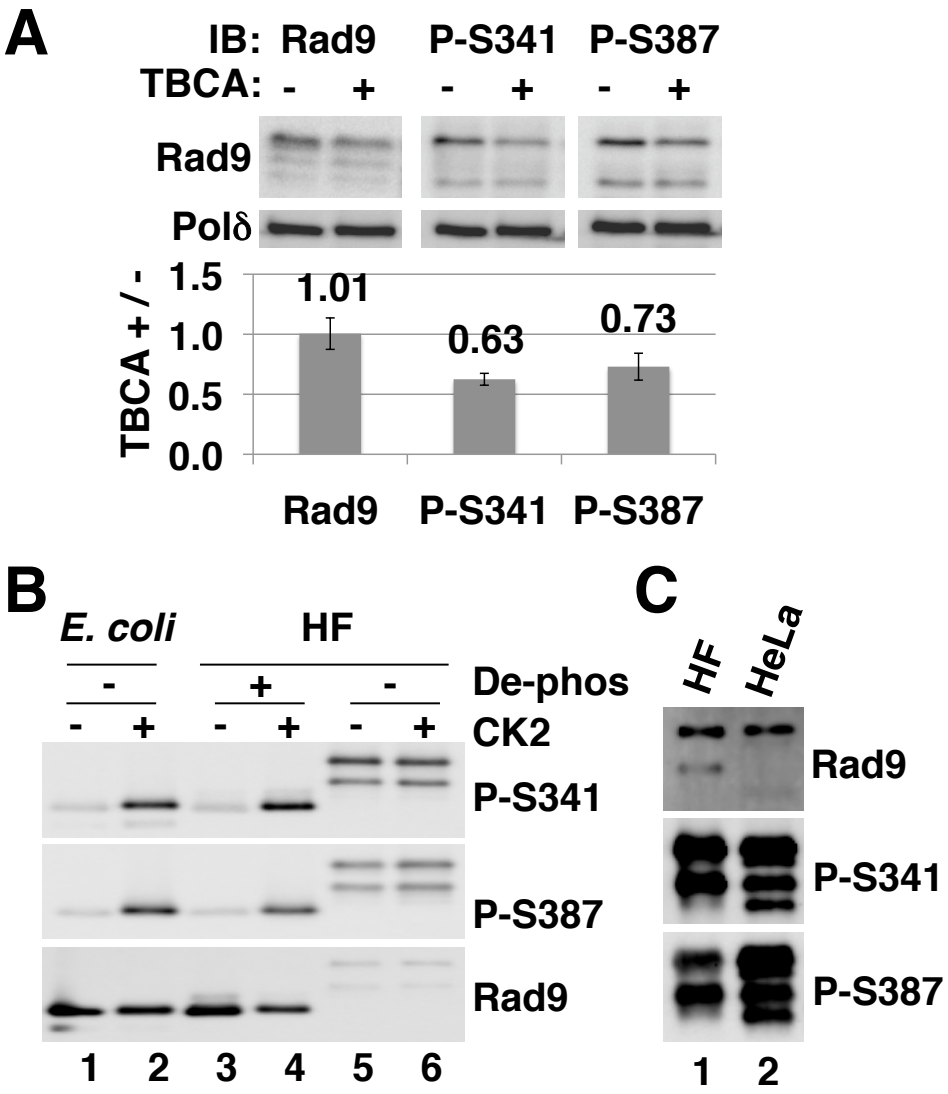
A
IB: Rad9 P-S341 P-S387
TBCA: - + - + - +
Rad9
Polδ
TBCA + / -
1.5
1.0
0.5
0.0
1.01
0.63
0.73
Rad9 P-S341 P-S387
B
E. coli
HF
-
+
-
De-phos
- + - + - +
CK2
P-S341
P-S387
Rad9
1 2 3 4 5 6
C
HF
HeLa
Rad9
P-S341
P-S387
1 2

Fig. 3

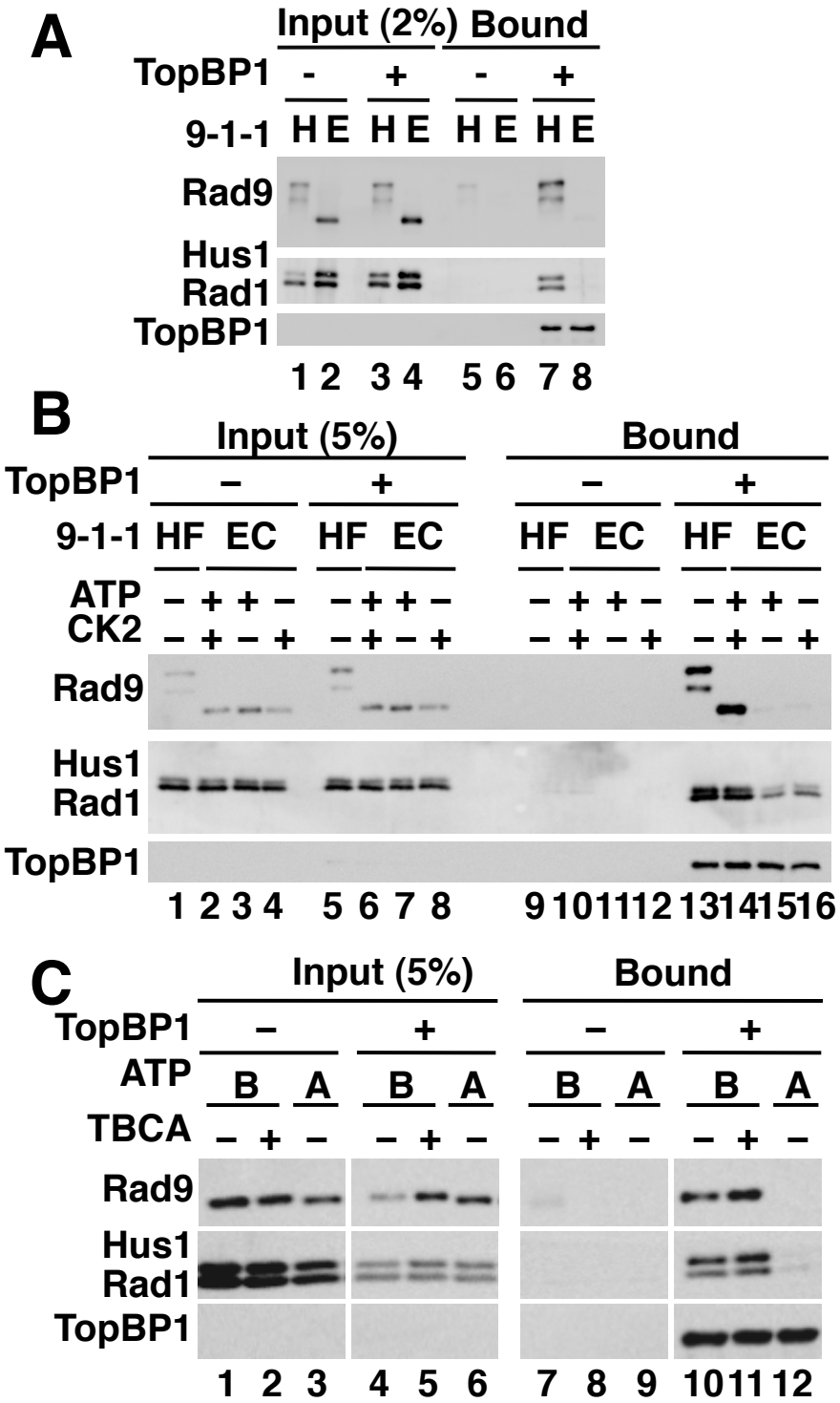
A
Input (2%)
Bound
TopBP1
-
+
-
+
9-1-1
H E H E H E H E
Rad9
Hus1
Rad1
TopBP1
1 2 3 4 5 6 7 8
B
Input (5%)
Bound
TopBP1
–
+
–
+
9-1-1
HF EC HF EC HF EC HF EC
ATP
CK2
Rad9
Hus1
Rad1
TopBP1
1 2 3 4 5 6 7 8 9 10 11 12 13 14 15 16
C
Input (5%)
Bound
TopBP1
–
+
–
+
ATP
B A B A B A B A
TBCA
Rad9
Hus1
Rad1
TopBP1
1 2 3 4 5 6 7 8 9 10 11 12

Fig. 4

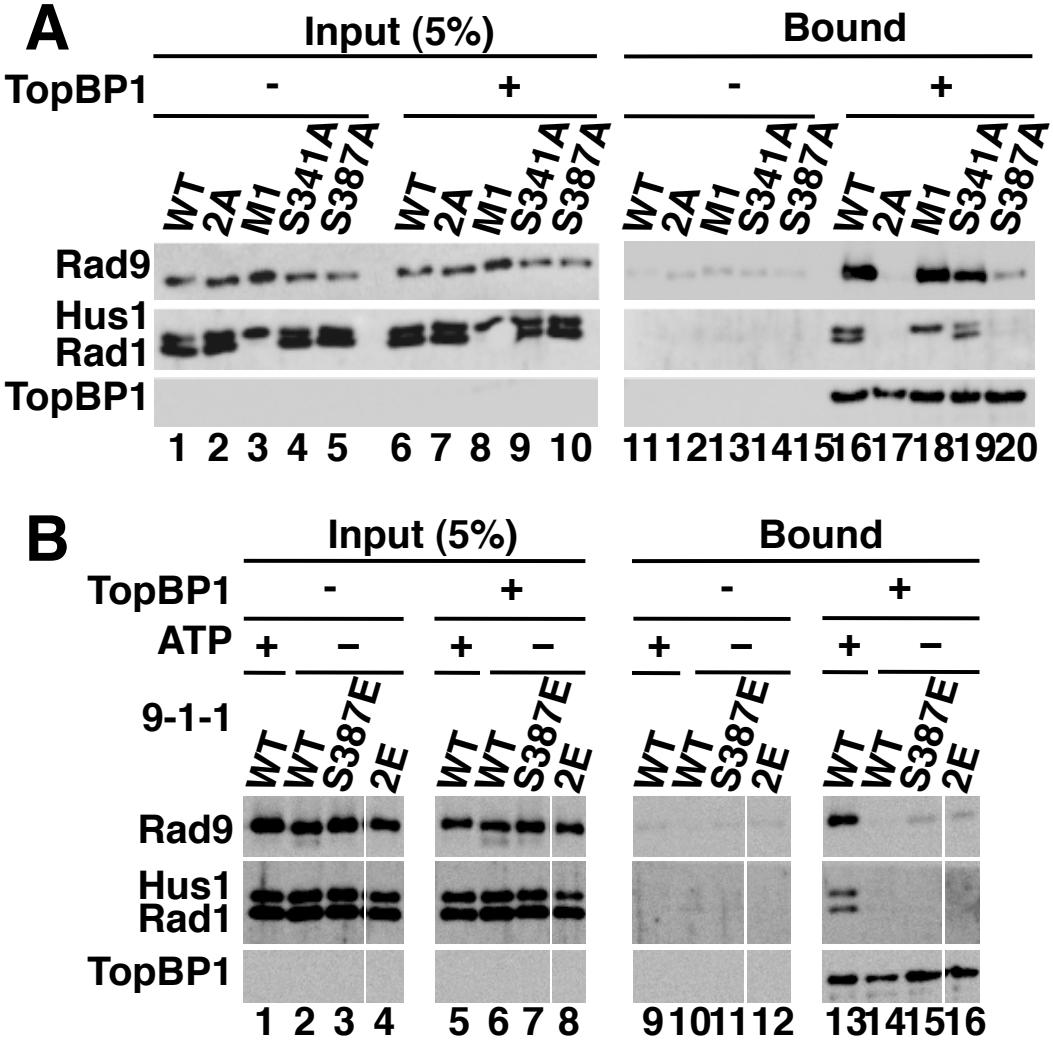
A
Input (5%)
Bound
TopBP1
-
+
-
+
WT
2A
M1
S341A
S387A
Rad9
Hus1
Rad1
TopBP1
1 2 3 4 5 6 7 8 9 10 11 12 13 14 15 16 17 18 19 20
B
Input (5%)
Bound
TopBP1
-
+
ATP
+
–
9-1-1
WT
WT
S387E
2E
Rad9
Hus1
Rad1
TopBP1
1 2 3 4 5 6 7 8 9 10 11 12 13 14 15 16

Fig. 5

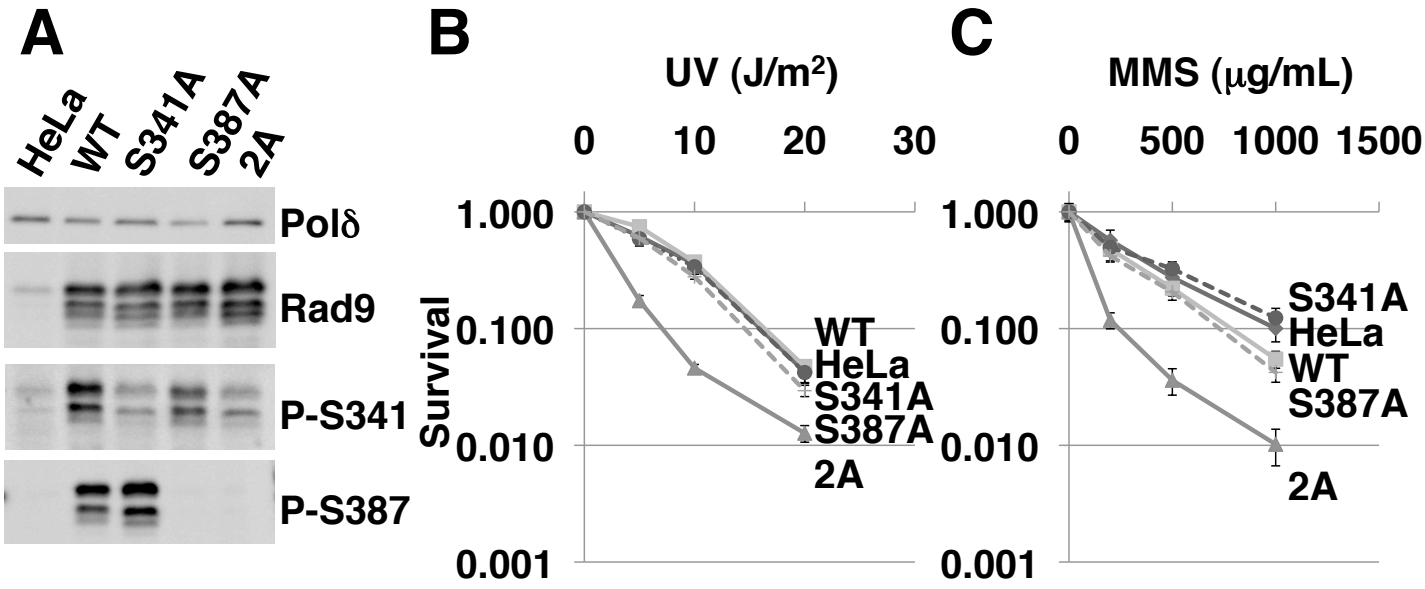
A
HeLa
WT
S341A
S387A
2A
Polδ
Rad9
P-S341
P-S387
B
UV (J/m2)
0
10
20
30
1.000
0.100
0.010
0.001
Survival
WT
HeLa
S341A
S387A
2A
C
MMS (μg/mL)
0
500
1000
1500
1.000
0.100
0.010
0.001
S341A
HeLa
WT
S387A
2A

Figure S1

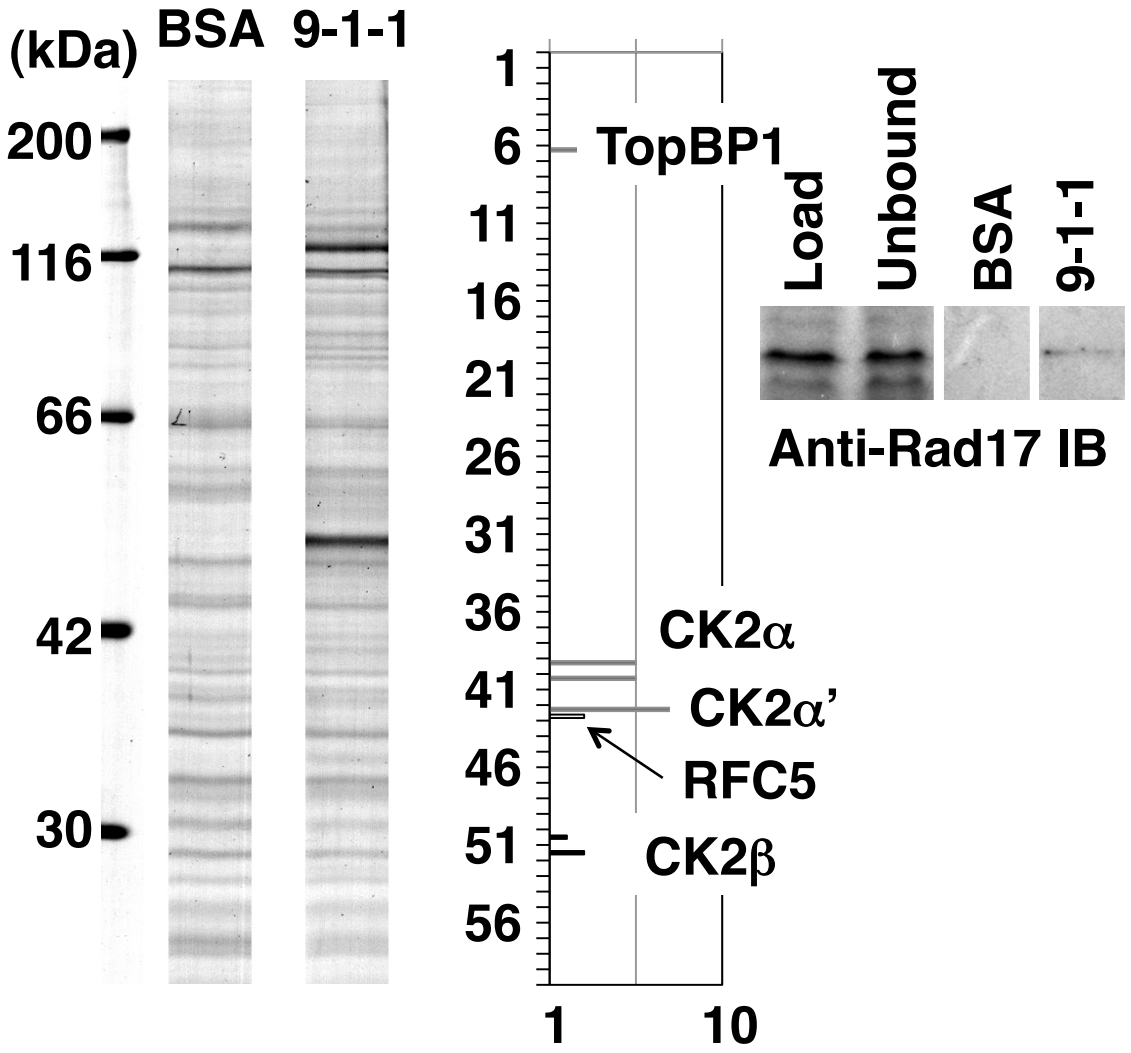
(kDa)
BSA
9-1-1
200
116
66
42
30
1
6
11
16
21
26
31
36
41
46
51
56
TopBP1
CK2α
CK2α'
RFC5
CK2β
1
10
Load
Unbound
BSA
9-1-1
Anti-Rad17 IB

Figure S2

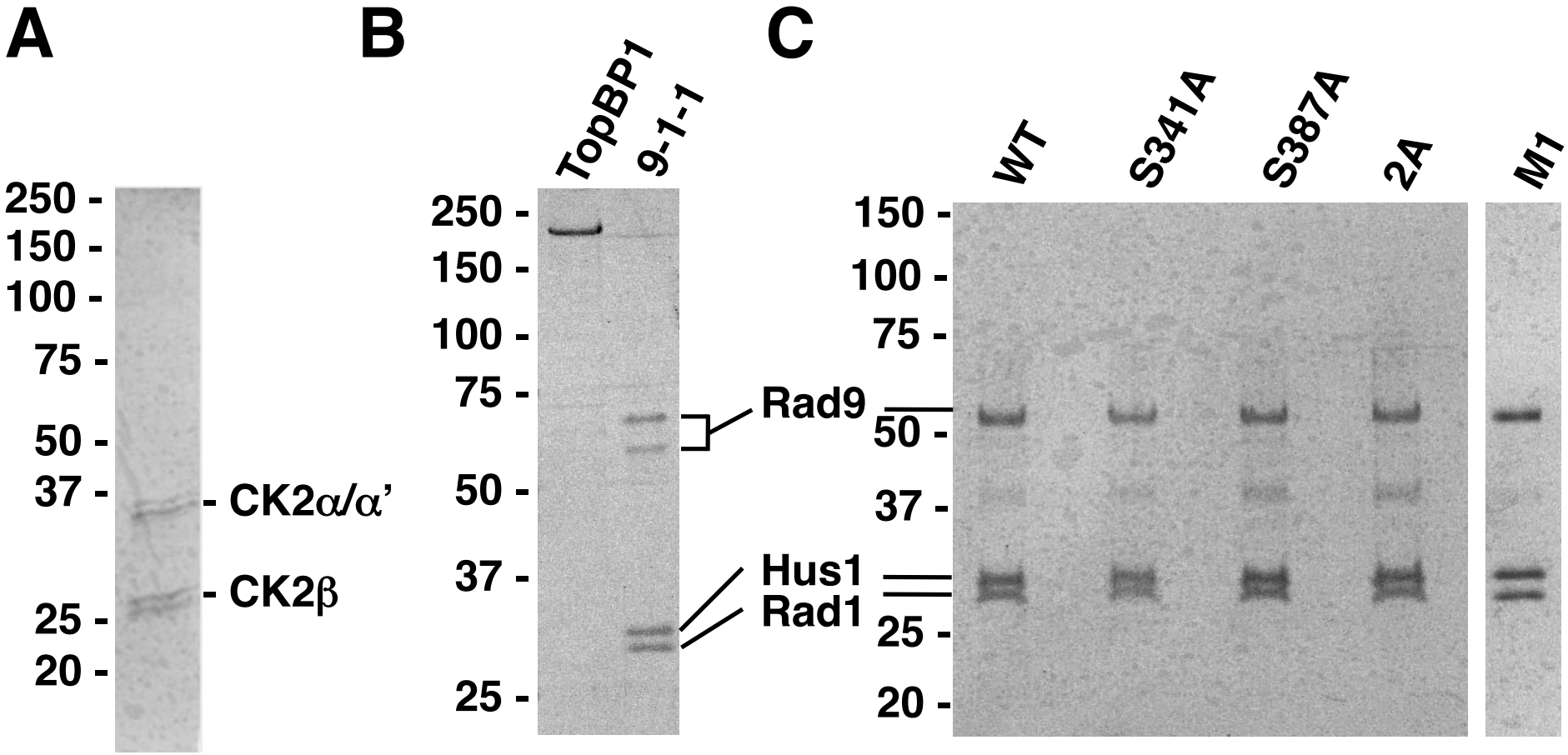
A
250 -
150 -
100 -
75 -
50 -
37 -
25 -
20 -
CK2α/α'
CK2β
B
TopBP1
9-1-1
250 -
150 -
100 -
75 -
50 -
37 -
25 -
Rad9
Hus1
Rad1
C
WT
S341A
S387A
2A
M1
150 -
100 -
75 -
50 -
37 -
25 -
20 -

Figure S3


Rad9
S341
hsRad9 IDS-YMIAMETTIGNEGSRVLPSISLSPGPQPPKSPGPH-SEEEDEAEPSTVPGTPPP 358
mmRad9 IDC-YMIAMETTGGNEGSGAQPSTSLPPVSLASHDLAP-ISEEE--AEPSTVPGTPPP 356
xlRad9 ID--YMIAMETTLANPSPPTSPTFCNRSSIIPLQESQGLSSDDE--LE-TGVPGTPPN 346
ggRad9 LES-YMVALESSACEGEAGAPPSPNFS-----LHTPRPAESDPEEEED-GAVPGTPPH 342
spRad9 HNPPGSIGWQTDQSDSSRMFNSALDRSDETNGIKEPSTTNDAGQSLFL-DGIPNESEL 396
scDdc1 IGTTHEVACPRNESNSLKRSIADICNETEDPTQQSTFAKRADTTVTWG-KALPAADDE 554
S387
hsRad9 KKFRSLFFGSILAPVRSPQGP-SPVLAEDSEGEG---------- 391
mmRad9 KKFRSLFFGSILAPVHSPQGP-NPVLAEDSDGEG---------- 389
xlRad9 KKFRSLFFGSILA--SSGHSN-QEILAEDSDGEE---------- 377
ggRad9 KKFRSLFFGSVLTPGGPGPAPSQEVLAEDSDAEC---------- 376
spRad9 AAFNNDVNDDAEFGPTQAEQSYHGIFSQED---------- 426
scDdc1 VSCSNIDRKGMLKKEKLKHMQGLLNSQNDTSNHKKQDNKEMEDGLGLTQVEKPRGIFD 599
Rad1
1 MPLLTQQIQD EDDQYSLVAS LDNVRNLSTI LKAIHFREHA TCFATKNGIK VTVENAKCVQ
61 ANAFIQAGIF QEFKVQEESV TFRINLTVLL DCLSIFGSSP MPGTLTALRM CYQGYGYPLM
121 LFLEEGGVVT VCKINTQEPE ETLDFDFCST NVINKIILQS EGLREAFSEL DMTSEVLQIT
181 MSPDKPYFRL STFGNAGSSH LDYPKDSDLM EAFHCNQTQV NRYKISLLKP STKALVLSCK
241 VSIRTDNRGF LSLQYMIRNE DGQICFVEYY CCPDEEVPES ES 282
S280 S282
S/T Acidic

Figure S4

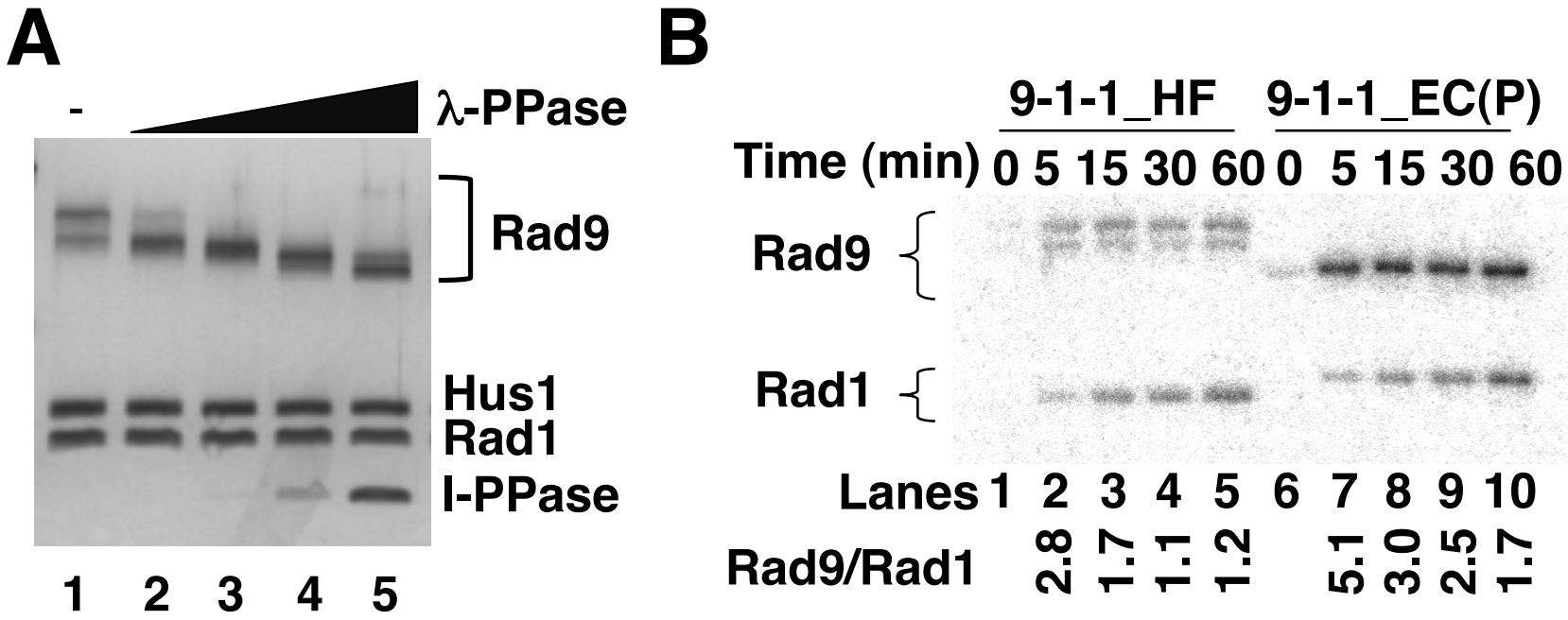
A
-
λ-PPase
Rad9
Hus1
Rad1
I-PPase
1 2 3 4 5
B
9-1-1_HF
9-1-1_EC(P)
Time (min) 0 5 15 30 60 0 5 15 30 60
Rad9
Rad1
Lanes 1 2 3 4 5 6 7 8 9 10
Rad9/Rad1 2.8 1.7 1.1 1.2 5.1 3.0 2.5 1.7

Figure S5

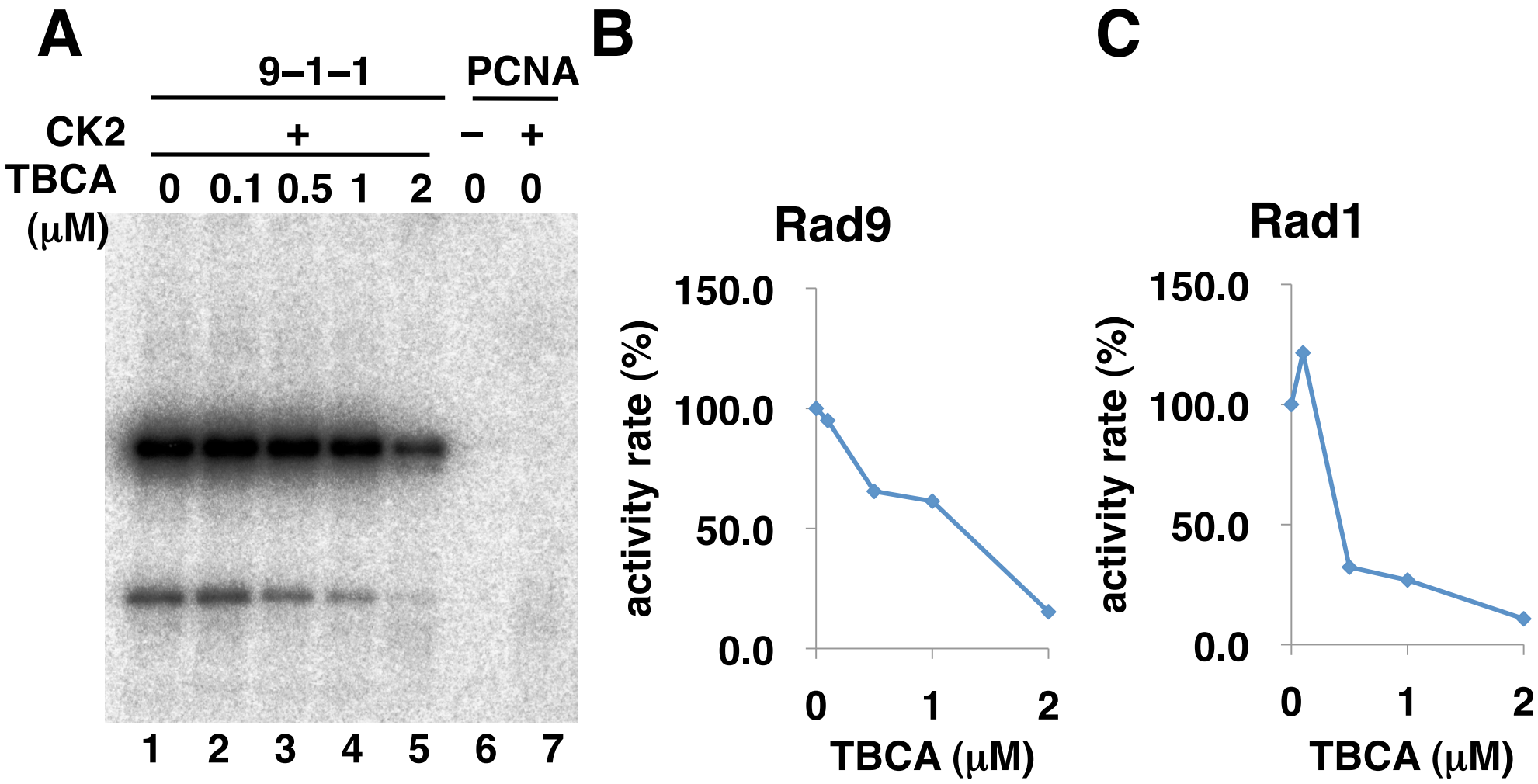
A
9–1–1
PCNA
CK2
+
– +
TBCA
0 0.1 0.5 1 2 0 0
(μM)
1 2 3 4 5 6 7
B
Rad9
activity rate (%)
150.0
100.0
50.0
0.0
0 1 2
TBCA (μM)
C
Rad1
activity rate (%)
150.0
100.0
50.0
0.0
0 1 2
TBCA (μM)

Figure S6

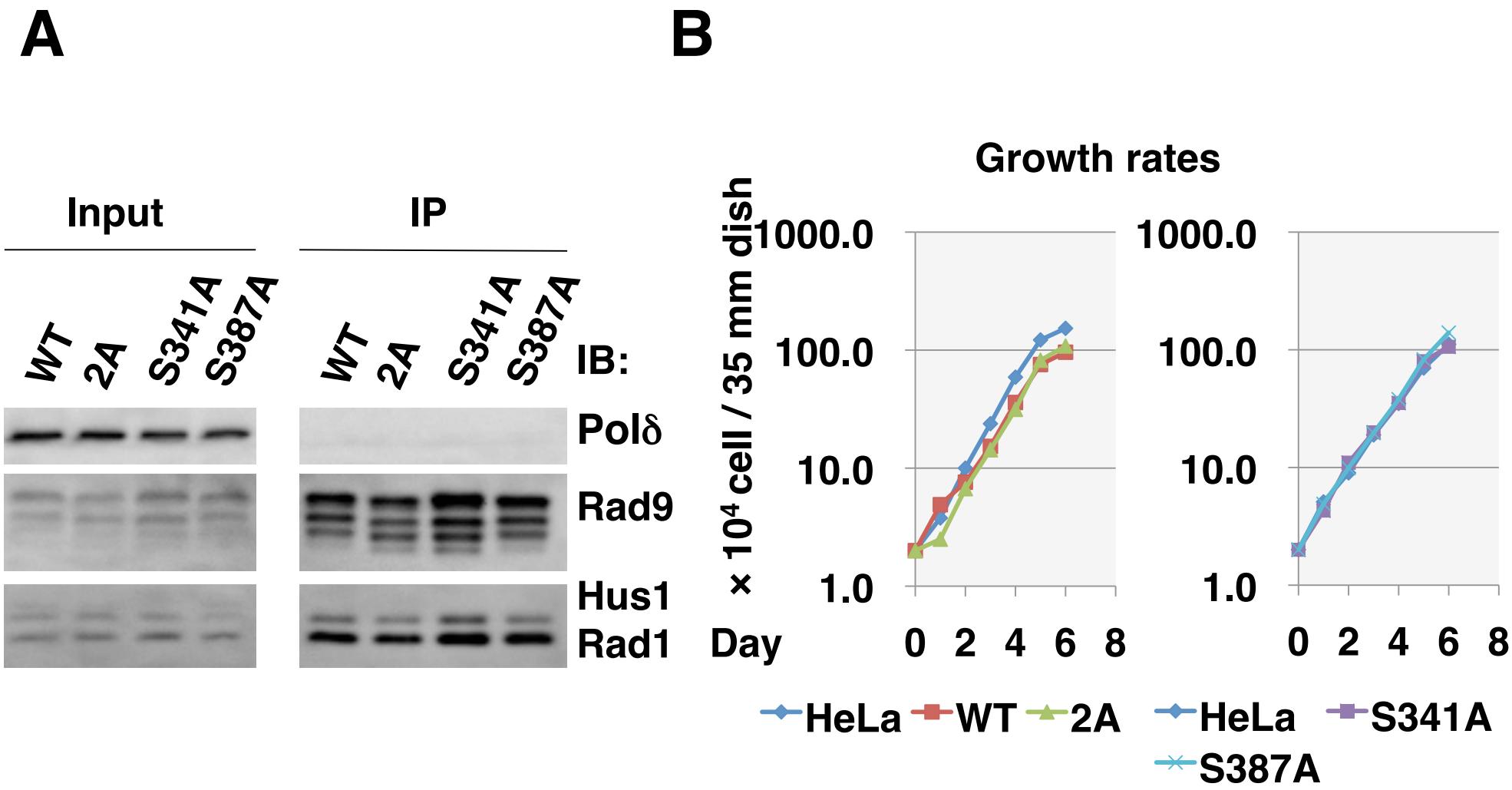
A
Input
IP
WT
2A
S341A
S387A
WT
2A
S341A
S387A
IB:
Polδ
Rad9
Hus1
Rad1
B
Growth rates
× 10⁴ cell / 35 mm dish
1000.0
100.0
10.0
1.0
Day
0 2 4 6 8
1000.0
100.0
10.0
1.0
0 2 4 6 8
HeLa
WT
2A
HeLa
S341A
S387A

Figure S7

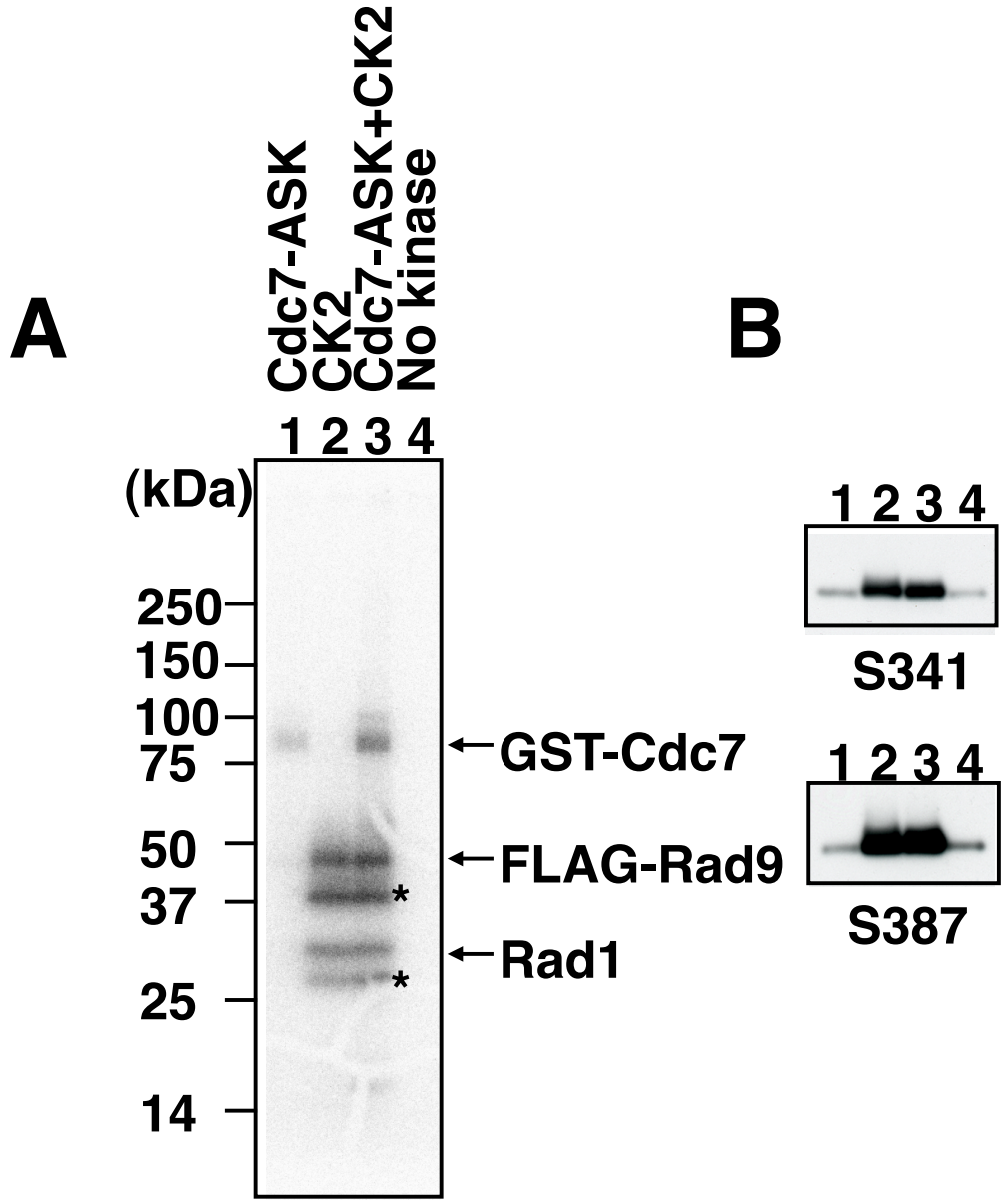
A
Cdc7-ASK
CK2
Cdc7-ASK+CK2
No kinase
1 2 3 4
(kDa)
250
150
100
75
50
37
25
14
GST-Cdc7
FLAG-Rad9
Rad1
*
*
B
1 2 3 4
S341
1 2 3 4
S387

Figure S8

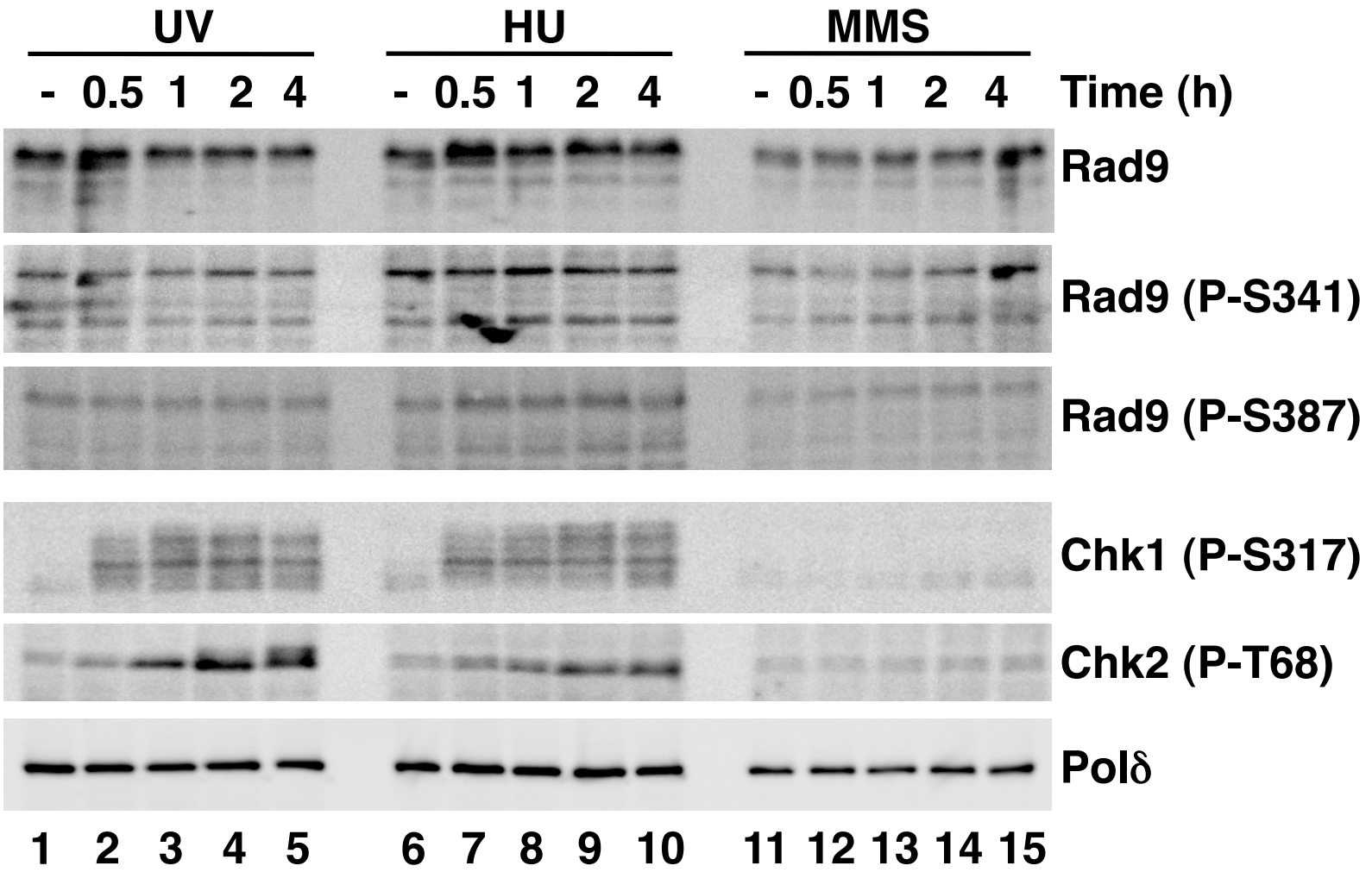
UV
HU
MMS
- 0.5 1 2 4
- 0.5 1 2 4
- 0.5 1 2 4
Time (h)
Rad9
Rad9 (P-S341)
Rad9 (P-S387)
Chk1 (P-S317)
Chk2 (P-T68)
Polδ
1 2 3 4 5 6 7 8 9 10 11 12 13 14 15